Light-scattering measurement of the nematic correlation length in a liquid crystal with quenched disorder

Tommaso Bellini,[1,4,*] Noel A. Clark,[2] Vittorio Degiorgio,[1,4] Francesco Mantegazza,[3,4] and Giorgio Natale[1,2]

[1]*Dipartimento di Elettronica Università di Pavia, 27100 Pavia, Italy*
[2]*Condensed Matter Laboratory, University of Colorado, Boulder, Colorado 80309-0390*
[3]*Istituto di Scienze Farmacologiche, Università di Milano, 20133 Milano, Italy*
[4]*Istituto Nazionale per la Fisica della Materia, 27100 Pavia, Italy*

We have studied a composite system formed by a nematic thermotropic liquid crystal in which small silica particles have been dispersed. The colloids are aggregated and exert a randomizing effect on the nematic structure. The distorted pattern of the optical axis gives rise to a strong optical turbidity τ. We have measured τ as a function of the silica concentration Φ and of the temperature T in both the isotropic and nematic phase. We have found that, at fixed T, τ has a maximum as a function of Φ, and that, upon changing Φ, the whole shape of $\tau(T)$ drastically transforms. We have devised a model to describe the scattering of light from a distorted uniaxial system. The model has been developed both in the Born approximation and in the anomalous diffraction approximation, the two regimes which cover the broad range of experimental conditions. The family of $\tau(T)$ curves experimentally obtained at different Φ's is remarkably well described by the theoretical model, using as the only fitting parameter the correlation length ζ. We have found that, upon decreasing Φ, the nematic correlation length diverges as a power law of Φ. We compare the exponent of the power law with the prediction of the Imry-Ma theory of phase behavior in disordered systems, and we discuss the connection between ζ and the fractal correlation length of the silica aggregates. [S1063-651X(98)14802-X]

PACS number(s): 61.30.Eb, 64.70.Md, 82.70.Gg, 78.35.+c

I. INTRODUCTION

Nematic liquid crystals containing dispersed colloidal particles, sometimes called ''filled nematics'' (FN), are attracting a growing interest in soft condensed matter physics, and have been the subject of a few different experimental studies [1,2]. Their interest is both fundamental and applicative. The fundamental physical interest of FN is connected to the study of phase transitions in the presence of controllable quenched disorder, which constitutes a kind of novel thermodynamical variable. Phase diagrams of liquid crystal (LC) as a function of the ''disorder density'' have already been theoretically introduced [3]. The fact that the amount of quenched disorder can be experimentally controlled in a FN has been clearly demonstrated by studying the calorimetric behavior at both the isotropic to nematic and nematic to smectic-*A* phase transitions: critical exponents, latent heat, finite size rounding effects, all depend on the concentration of silica particles in a continuous fashion [2]. The applicative interest stems from the fact that the strong optical opacity of the FN can be suppressed by the application of an external electric field, which couples with the nematic director and forces an overall alignment of the LC overriding the quenched disorder. This forced alignment persists, as a metastable state, even when the field is removed. The scattering state can be reproduced by locally heating the system over the clearing temperature and then letting it go back to the nematic phase [1].

This phenomenon has been exploited to realize prototypes of reversible optical memories, whose readability is a consequence of the difference in the total scattering between the oriented phase and the distorted nematic phase.

We have studied a liquid crystal in which we have dispersed small silica particles commercially available in powder form (Aerosil). When these particles are dispersed in the LC in concentrations above the fraction of percent, they aggregate and form gel-like structures [1]. The LC molecules in contact with the silica surface experience a local field which usually strongly favors an alignment parallel to the interface [4]. Since the aggregated colloids have a random structure, such a local field has an overall randomizing effect on the nematic director. A randomizing field fixed in space, depending neither on temperature nor on the phase structure of the LC, such as the one described here, is generally referred to as ''quenched disorder.'' The structure of the nematic phase in the composite LC-Aerosil system is then the consequence of a compromise between the quenched disorder provided by the silica particles and the elastic force which tends to minimize the distortions of the nematic director. The result is a disordered nematic phase, in which the orientation of the nematic director, and hence of the optical axis, is continuously distorted as a function of the position in the system. The quality of the local orientational order, expressed by the local nematic order parameter, is presumably constant, since the distortions induced by the silica particles have a spatial range much larger than the molecular size.

The composite LC-Aerosil system we have studied is a weak scatterer when the LC is in the isotropic phase, but becomes highly opaque (much more than the bulk nematic) when the LC is in the nematic phase. Due to the large birefringence of the nematic phase, the spatial fluctuations in the

---

*Author to whom correspondence should be addressed. Address correspondence to Dipartimento di Elettronica, Università di Pavia, via Ferrata 1, 27100 Pavia, Italy.

orientation of the optical axis strongly scatter light. Measuring the turbidity is then a way to quantitatively evaluate the nematic distortions.

This work focuses on the measurement of the nematic correlation length ζ in the FN, i.e., the correlation length for the spatial fluctuations in the nematic orientation. As discussed below, in our system ζ can also be defined as one-third of the correlation length for the director autocorrelation function $g(R)$ which is assumed to be exponential:

$$g(R) = \langle \mathbf{n(r)} \cdot \mathbf{n(r+R)} \rangle = \exp(-R/3\zeta), \qquad (1)$$

where $n(\mathbf{r})$ is the unit vector representing the nematic director at a given position $\mathbf{r}$, $R = |\mathbf{R}|$. $\langle\,\rangle$ indicates averaging over the $\mathbf{r}$ position. We assume that $g(R)$ is isotropic. This is reasonable, given the isotropic nature of the quenched disorder produced in the system.

ζ is a quantity of key importance for the understanding of the phase transition in the presence of disorder. ζ is in fact a direct measure of the ''resistance'' or the ''stability'' of the nematic phase to the presence of quenched disorder. In principle, ζ can be larger than the typical length over which the disordering structure is correlated. The study of the dependence of ζ on the density of disorder may constitute an experimental verification of the Imry-Ma argument [5], a cornerstone in the statistical physics of disordered systems. Moreover, as far as applications are concerned, both the optical turbidity, and therefore the contrast of the FN applications, and the electric field threshold for switching depend on ζ.

In the work presented here, we have measured the optical turbidity τ of a FN as a function of the volume fraction Φ of the dispersed silica particles and of the temperature T. We have devised a model suitable to describe the scattering of light from a distorted uniaxial system. The model has been developed both in the Born approximation and in the anomalous diffraction approximation, the two regimes encountered under the experimental conditions. Our model describes remarkably well the family of $\tau(T)$ curves experimentally obtained for different values of Φ. We show that the measurement of the optical turbidity τ of a FN as a function of temperature T enables us to derive with good precision the value of the nematic correlation length. The observed dependence of ζ on Φ is discussed in terms of the fractal properties of the silica gel and of available theoretical results on the effect of disorder on phase transitions.

This paper is organized as follows. In Sec. II we describe the experiment and present the results. Sections III and IV are devoted to the light-scattering models, developed, respectively, in the Born approximation and in the anomalous diffraction approximation. In Sec. V we compare the experimental results to the models, deriving ζ for the different samples used in the experiment and discussing the scaling behavior we find. In Sec. VI we state our conclusions.

II. EXPERIMENTAL METHODS AND RESULTS

The experiment was performed with the thermotropic liquid crystal hexacyanobiphenyl (6CB). 6CB is a well characterized LC [6]. Its phase diagram exhibits isotropic (I), nematic (N), and crystal (X) phases as follows:

$$X \xrightarrow[T_{XN}=14.5\,°C]{} N \xrightarrow[T_{NI}=28.8\,°C]{} I.$$
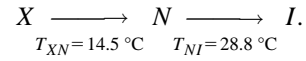
In the nematic phase the molecules display a long range orientational order along a common direction, named the nematic director. The onset of a preferential direction for the molecular axis makes the nematic phase anisotropic in its most relevant physical properties. Optically, the nematic phase can be described as a uniaxial material, having a temperature-dependent birefringence [7]. We call $m_\parallel$ and $m_\perp$, respectively, the refractive indices parallel and perpendicular to the nematic director $\mathbf{n}$. The birefringence, defined as $\Delta m = m_\parallel - m_\perp$, upon lowering the temperature has a discontinuous increase at the first-order transition temperature T_{NI} to a value about $\Delta m = 0.10$. By further lowering T, Δm continuously grows and reaches a value of $\Delta m = 0.16$ when $T = T_{XN}$ [6(a)]. Apart from a small temperature interval around T_{NI}, the birefringence of the nematic phase can usually be described by using the phenomenological expression $\Delta m = \Delta m_0 (T_{NI} - T)^\beta$ [8]. In the case of bulk 6CB, we have fitted the data presented in Ref. [6(a)] and found $\Delta m_0 = 0.107$ and $\beta = 0.166$.

The samples have been prepared by dispersing Degussa Aerosil R812 silica nanoparticles in the 6CB. The Aerosil R812 is a colloid with a globular shape, its size distribution for the diameter is peaked at 7 nm and presents a half-width of about 2 nm [9]. The Aerosil colloids are produced under flame in the form of powder and used industrially as thickeners. We have chosen the Aerosil R812 because it is treated to lower the concentration of silanol groups on the surface and therefore to reduce its hydrophilic character. This fact, according to our experience, increases the stability of the FN mixture, especially at low concentrations of silica.

The samples have been prepared both by direct dispersion and by dispersion in an intermediate solvent which was subsequently evaporated at a temperature above T_{NI}. The volume fraction of silica particle used in our experiment covers the range 0.009–0.25. To check whether the silica particles in the LC are aggregated, we have performed dynamic light-scattering measurements in the isotropic phase. We have found indeed that the measured translational diffusion coefficient corresponds to that of a 10 μm diameter aggregate. For the present work, which does not deal with the physics of the dispersion, but is instead focused on the resulting distorted uniaxial structure, what is important is the fact that the Aerosil is aggregated in some sort of colloidal gel, and therefore presumably does not appreciably change its structure when the LC undergoes a phase transformation.

The experiments have been performed by putting the samples into thin cells made with semioptical glass, treated on the surface so as to favor perpendicular alignment of the molecules. We have used cells having thickness $d = 20$ and 50 μm, depending on the value of τ.

In order to measure the transmitted intensity, we have used a standard procedure, i.e., we have illuminated the FN cell by a He-Ne laser expanded beam and we have tightly selected the light exiting the cell in the forward direction by a small pin hole on the focal plane of a converging lens. The temperature was set by a computer interfaced Instec RTC-1 temperature controller. The temperature stability is of the order of $(2 \times 10^{-3})\,°C$. The experimental runs were per-
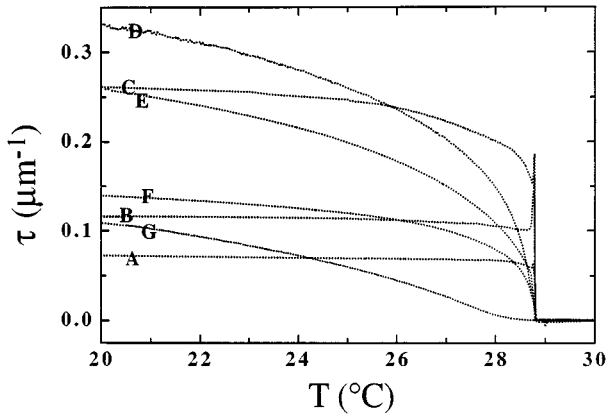
FIG. 1. Optical turbidity τ measured as a function of the temperature T for different values of the silica volume fraction Φ. The alphabetic sequence in the labels of the curves $A-G$ is for increasing values of Φ. Curve A: $\Phi=0.009$; curve B: $\Phi=0.013$; curve C: $\Phi=0.026$; curve D: $\Phi=0.052$; curve E: $\Phi=0.083$; curve F: $\Phi=0.120$; curve G: $\Phi=0.254$.

formed by using temperature ramps of about 0.8 °C/h. The value of τ has been derived from the measurements according to the extinction equation

$$I_T=I_0 \exp[-\tau d], \tag{2}$$

where I_0 and I_T are, respectively, the incident and the transmitted intensity.

It should be stressed that the validity of Eq. (2) is not limited to the single-scattering regime. It can be used also in a situation in which multiple scattering is relevant, provided that the forward scattered intensity is small in comparison to the transmitted intensity. The minimum value of the ratio I_T/I_0 which, for our optical setup, is acceptable in order to have a negligible contribution from the scattered intensity is about $I_T/I_0=10^{-3}$.

In Fig. 1 we show some curves of τ vs temperature T measured with samples containing different volume fractions Φ of silica particles. It can be easily noted that, upon increasing Φ, there are considerable changes in the shape of the temperature dependence of τ. This fact indicates that the shape of $\tau(T)$ is a nontrivial feature of the FN, and therefore it can be used as a probe of the internal structure of the system.

Three different regimes, of low, intermediate, and high Φ, can be easily recognized by a first inspection of Fig. 1.

(1) A low Φ regime (roughly $0.009<\Phi<0.055$), where, for growing values of Φ we obtain growing values of τ. In this regime, upon lowering T, τ has a large increase at $T=T_{NI}$ and an almost saturated behavior for lower T. Also notice the presence of a peak at $T=T_{NI}$. Such a peak is a nonequilibrium feature of the system, and can be removed by letting the system thermalize for long enough time. Curves A, B, and C belong to this regime of concentrations.

(2) An intermediate Φ regime (roughly $0.055<\Phi<0.2$), where, for growing values of Φ, we obtain decreasing values of τ. In this regime, the behavior at the transition remains discontinuous, τ is rather strongly dependent on T in the whole nematic range, and the peak at $T=T_{NI}$ is absent. In this regime the τ vs T curves are all similar in shape and

compare well with the T dependence of the bulk Δm^2. Curves D, E, and F belong to this regime of concentrations.

(3) A high Φ regime ($\Phi>0.2$), where, for growing values of Φ, τ decreases as in the previous regime, but displays a continuous behavior at the NI phase transition. Also notice the fact that, in this regime, the apparent T_{NI} decreases for increasing Φ. The behavior of the FN in this regime contains all the elements predicted and observed for the NI transition of LC in random environments [10]. Curve G belongs to this regime of concentrations.

III. LIGHT SCATTERING FROM A DISTORTED NEMATIC: BORN APPROXIMATION

In order to interpret the experimental results, we have developed a quantitative model for the calculation of the light-scattering cross section. The turbidity is simply derived by performing an integral over all possible directions of the differential scattering cross section of the medium. As such, τ is a property only of the medium, independent from geometry and size of the sample.

Our model assumes that the orientation of the nematic director presents spatial fluctuations with a scalar order parameter which is constant throughout the sample, that is, the scattering medium is a uniaxial material having continuous but random distortions of the optical axis. This situation is different from the standard problem of light scattering from a bulk LC. Many theoretical treatments have been presented describing the scattering of light from the isotropic phase in the proximity of the NI transition [11], or from the nematic phase [7]. In such cases the main contribution to the scattered light comes from the spontaneous fluctuations of the scalar order parameter due to thermal motion. On the contrary, in the FN the main contribution to scattering comes from the large spatial fluctuations introduced by the quenched disorder, whereas thermal fluctuations can be neglected in our approach. The available theoretical treatments which are closer to our experimental situation are those concerning the light scattered by anisotropic particles in a homogeneous medium [12], in particular those referring to uniaxial scatterers having sharp boundaries (colloids, LC droplets, and LC domains) [13].

In this section and in the following we present calculations of the total scattering cross section performed in the frame of two different approximations: the weak scattering approximation, or Born approximation (BA), and the anomalous diffraction approximation (ADA) [12]. These approximations become exact in two different limiting regimes, defined in terms of amplitude and spatial extension of the fluctuations of refractive index. When one deals with scattering from homogeneous particles in a homogeneous medium, the amplitude of the fluctuations of the refractive index is given by the difference between the refractive indices of particle and solvent, while the typical size of the fluctuations is given by the particle radius. In our case, instead, amplitude and size of the fluctuations are given, respectively, by the birefringence Δm and nematic correlation length ζ. The BA, also called the Rayleigh-Gans approximation when dealing with scattering from particles, is valid in the regime where $\Delta m \ll 1$ and $\zeta \Delta m \ll \lambda$. The ADA, instead, is valid when

$\Delta m \ll 1$ and $\zeta \gg \lambda$. As discussed below, the two regimes have a region of overlap.

The common ground for the development of the two models is the twofold assumption already introduced in Sec. I: the validity of Eq. (1) and the fact that the local birefringence of the LC is equal to the bulk Δm. This latter assumption is indeed a very reasonable one since the director distortions are on a length scale much larger than the molecular size. The way we have modeled the system in order to perform the calculations of the total scattering is different in the two approximations. While in the BA calculation we use only the statistical properties of the continuous distortion of the nematic director, in the ADA calculation we make a more drastic assumption: we assume that our system is a collection of independent anisotropic scatterers having a birefringence which decays to zero as one moves away from their centers. We discuss now the BA approximation which essentially requires that the phase change of the optical field over a distance comparable with the range of fluctuations is much smaller than 2π. Within such an approximation, the average scattered intensity is simply proportional to the spectral components of the dielectric tensor $\epsilon_{\alpha\beta}(\mathbf{r})$. This fact makes possible the derivation of the differential scattering cross section from the statistical properties of the director.

Let us consider a volume V illuminated by a monochromatic beam polarized along x ($\mathbf{u}_x$ is the unit vector along x), and propagating in the direction z. We call I_0 the intensity of the incident beam, λ the wavelength, $k_0 = 2\pi\langle m\rangle/\lambda$. Let us assume that the scattered intensity is collected at a distance L from the scattering volume (where L is much larger than the size of the scattering volume), and that $\mathbf{u}_f$ is its polarization, let us make use of the ordinary Euler angles θ and ϕ around the z axis to describe the scattering direction (see Fig. 2), and let us call $\mathbf{k}_0$ and $\mathbf{k}_f$ the wave vectors of the incident and scattered light. The scattering vector $\mathbf{q} = \mathbf{k}_0 - \mathbf{k}_f$ has amplitude $q = 2k_0 \sin(\theta/2)$. The intensity $I_{x,f}(\mathbf{q})$ scattered per unit solid angle with polarization $\mathbf{u}_f$ is [14]

$$I_{x,f}(\mathbf{q}) = I_0 k_0^4 V |\epsilon_{x,f}(\mathbf{q})|^2 / (16\pi^2 L^2 \langle m\rangle^4), \qquad (3)$$

where $\epsilon_{x,f}(\mathbf{q}) = \mathbf{u}_x \cdot \underline{\underline{\epsilon}}(\mathbf{q}) \cdot \mathbf{u}_f$. The optical turbidity τ is calculated as

$$\tau = \int_0^{2\pi} d\phi \int_0^\pi d\theta L^2 I(\mathbf{q}) \sin\theta / (I_0 V), \qquad (4)$$

where $I(\mathbf{q}) = I_{x,f1}(\mathbf{q}) + I_{x,f2}(\mathbf{q})$, $\mathbf{u}_{f1}$ and $\mathbf{u}_{f2}$ being two orthogonal polarization states.

We divide the calculation in two parts: in the first we detail the specific assumption used to calculate the spectral components $|\epsilon_{x,f}(\mathbf{q})|^2$, in the second we calculate the optical turbidity of the system.

A. Calculation of the spectral components of the dielectric tensor

We start by noting that, because of the assumed isotropy of the nematic correlation function, Eq. (1) can be expressed in terms of the director components

$$\langle n_\alpha(\mathbf{r}) n_\alpha(\mathbf{r}+\mathbf{R})\rangle \propto \exp(-R/3\zeta), \qquad (5)$$

where α indicates the x, y, or z direction in a Cartesian reference frame.

Let us call S the scalar nematic order parameter. Experimentally, S can be defined through its proportionality with the bulk LC birefringence

$$\Delta m(T) = \Delta m_s S(T), \qquad (6)$$

where Δm_s is the birefringence one would have in a nematic where all molecules were perfectly aligned along the director. It is also useful to define the saturated dielectric anisotropy at optical frequencies $\Delta\epsilon_s = \Delta(m_s^2) \approx 2\langle m\rangle\Delta m_s$.

The local tensorial order parameter $\underline{\underline{Q}}$ can than be written as [7]

$$Q_{\alpha\beta} = S(3n_\alpha n_\beta - \delta_{\alpha\beta})/2. \qquad (7)$$

The dielectric tensor is, in a nematic LC, basically proportional to Q [11],

$$\epsilon_{\alpha\beta}(\mathbf{r}) = \langle\epsilon\rangle\delta_{\alpha\beta} + \tfrac{2}{3}\Delta\epsilon_s Q_{\alpha\beta}(\mathbf{r}). \qquad (8)$$

From Eqs. (7) and (8) it follows that, to compute the spectral components of the dielectric tensor $|\epsilon_{\alpha\beta}(q)|^2$, we need to know $\langle n_\alpha(\mathbf{r})n_\beta(\mathbf{r})n_\alpha(\mathbf{r}+\mathbf{R})n_\beta(\mathbf{r}+\mathbf{R})\rangle$. Therefore the nematic correlation function in Eq. (5) is not sufficient and we need to introduce a further assumption on $\mathbf{n}(\mathbf{r})$. It is interesting to note that a similar problem is found in the description of the rotational diffusion of a Brownian particle presenting a symmetry axis. The difference between the two cases is that in the latter the origin of the noise is thermal and the direction of the particle axis is a time-dependent random variable, whereas in the case of the FN the noise is static and the nematic director is a space-dependent random variable. By taking advantage of the fact that the solution to the problem of the rotational Brownian motion of a uniaxial particle is known [14], we exploit the analogy by transporting in the spatial domain the solutions which are available in the time domain. If we consider a line cutting across the sample, and we call x the position along the line, we assume that the statistical properties of $\mathbf{n}(x)$ are the same as those of the unit vector describing the orientational Brownian motion of the particle axis as a function of time. A justification for such an approach may come from the observation that the correlation function for $\mathbf{n}(\mathbf{r})$ depends only on the modulus of the displacement $\mathbf{R}$, and is therefore a function of a unidimensional variable. However, in order to put on a firmer basis the light-scattering treatment, it would be useful to find a more realistic model which describes the distortions of a three-dimensional elastic medium when randomly pinned.

Once we substitute inside the solutions for the rotational Brownian motion the displacement in space to the time delay, and the spatial correlation range to the reciprocal of the rotational diffusion constant, the analogy gives the following expressions:

$$\langle n_\alpha(\mathbf{r}) n_\alpha(\mathbf{r}+\mathbf{R})\rangle = \tfrac{1}{3}\exp(-R/3\zeta), \qquad (9)$$

$$\langle n_\alpha(\mathbf{r}) n_\beta(\mathbf{r})\rangle = 0 \quad (\alpha\neq\beta), \qquad (10)$$

$$\langle n_\alpha^2(\mathbf{r}) n_\alpha^2(\mathbf{r}+\mathbf{R})\rangle = \tfrac{1}{9} + \tfrac{4}{45}\exp(-R/\zeta), \qquad (11)$$
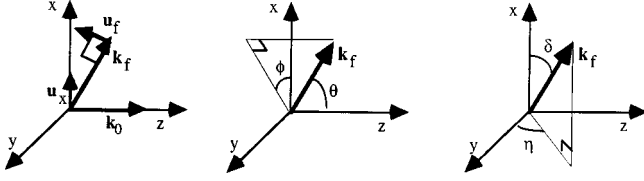
FIG. 2. Geometrical definitions of quantities used in the BA model. $\mathbf{k}_0$ and $\mathbf{k}_f$ are the wave vectors of the incident and scattered light. $\mathbf{u}_x$ and $\mathbf{u}_f$ are the polarizations of the incident and scattered light. θ, ϕ and δ, η are Eulerian angles defining the orientation of $\mathbf{k}_f$.

$$\langle n_\alpha(\mathbf{r})n_\beta(\mathbf{r})n_\alpha(\mathbf{r}+\mathbf{R})n_\beta(\mathbf{r}+\mathbf{R})\rangle = \tfrac{1}{15}\exp(-R/\zeta)$$

$$(\alpha \neq \beta). \qquad (12)$$

Note that Eqs. (9)–(11) incorporate the notion that $n_x^2(\mathbf{r})+n_y^2(\mathbf{r})+n_z^2(\mathbf{r})=1$. From Eq. (7) it follows that

$$\langle Q_{\alpha\alpha}(\mathbf{r})Q_{\alpha\alpha}(\mathbf{r}+\mathbf{R})\rangle = S^2\tfrac{1}{5}\exp(-R/\zeta), \qquad (13)$$

$$\langle Q_{\alpha\beta}(\mathbf{r})Q_{\alpha\beta}(\mathbf{r}+\mathbf{R})\rangle = S^2\tfrac{3}{20}\exp(-R/\zeta) \quad (\alpha \neq \beta), \qquad (14)$$

and therefore, from Eq. (8),

$$|\epsilon_{\alpha\alpha}(\mathbf{q})|^2 = \tfrac{32}{45}\pi S^2 \Delta\epsilon_s^2 \zeta^3 (1+q^2\zeta^2)^{-2}, \qquad (15)$$

$$|\epsilon_{\alpha\beta}(\mathbf{q})|^2 = \tfrac{8}{15}\pi S^2 \Delta\epsilon_s^2 \zeta^3 (1+q^2\zeta^2)^{-2} \quad (\alpha \neq \beta). \quad (16)$$

Equations (13) and (14), which express the correlation function for the nematic order parameter, justify our former definition of ζ as a ''nematic correlation length.'' Furthermore, Eqs. (15) and (16) show that ζ is also the relevant length for the fluctuation in the optical properties which results from the fluctuation in orientation of the optical axis.

B. Calculation of the scattered intensity

Let us call δ and η the Euler angles of the scattering direction referred to the x axis, as shown in Fig. 2. The Eulerian angles (θ, ϕ) and (δ, η) are connected as follows:

$$\cos\delta = \sin\theta\cos\phi,$$

$$\cos\eta = \sin\theta\sin\phi(1-\sin^2\theta\cos^2\phi)^{-1/2}. \qquad (17)$$

Given a scattering direction, we choose two perpendicular $\mathbf{u}_f$ directions as follows: $\mathbf{u}_{f1}$ lies in the plane defined by $\mathbf{u}_x$ and $\mathbf{k}_f$, while $\mathbf{u}_{f2}$ is perpendicular to it. Expressed in their components these two vectors are

$$\mathbf{u}_{f1} \equiv (u_{f1x}, u_{f1y}, u_{f1z})$$

$$= (\sin\delta, -\cos\delta\cos\eta, -\cos\delta\sin\eta), \qquad (18)$$

$$\mathbf{u}_{f2} \equiv (u_{f2x}, u_{f2y}, u_{f2z}) = (0, \sin\eta, -\cos\eta).$$

From Eq. (3) we then have

$$I_{x,f1}(\mathbf{q}) = I_0 k_0^4 V|\epsilon_{xx}(\mathbf{q})u_{f1x}+\epsilon_{xy}(\mathbf{q})u_{f1y}$$
$$+\epsilon_{xz}(\mathbf{q})u_{f1z}|^2/(16\pi^2 L^2\langle m\rangle^4), \qquad (19)$$
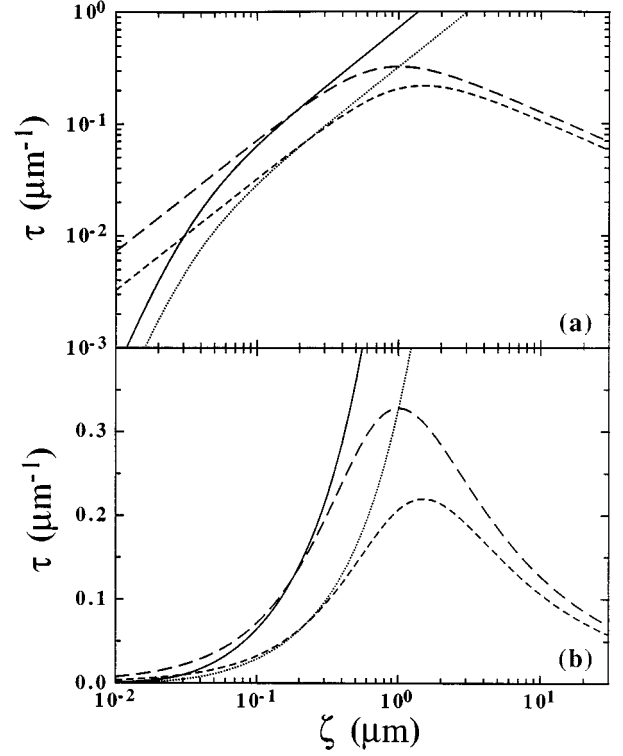
FIG. 3. Calculated values of the turbidity τ as a function of the nematic correlation length ζ according to the BA and ADA models, at two different temperatures, plotted in a log-log scale (a) and in a log-lin scale (b). Continuous line: BA model with $T=20\,°C$. Long dashed line: ADA model with $T=20\,°C$. Dotted line: BA model with $T=28\,°C$. Short dashed line: ADA model with $T=28\,°C$.

$$I_{x,f2}(\mathbf{q}) = I_0 k_0^4 V|\epsilon_{xy}(\mathbf{q})u_{f2y}+\epsilon_{xz}(\mathbf{q})u_{f2z}|^2/(16\pi^2 R^2\langle m\rangle^4). \qquad (20)$$

The quantities $\epsilon_{\alpha\beta}(\mathbf{q})$ are in general complex. Equation (20) yields the whole speckled structure of the scattered light. The phases are specific to the particular system realization. By assuming ensemble averaging, Eqs. (19) and (20) greatly simplify. The ensemble average is realized when the collected area is larger than a coherence area. In a geometry suitable for $I(\mathbf{q})$ measurements, where the incident beam is not focused, or even is deliberately enlarged, such a speckle average is always performed. In particular, this is obviously true when the optical turbidity is measured. After ensemble averaging, and making use of the isotropy assumption, we obtain

$$|\epsilon_{x,f1}(\mathbf{q})|^2 = |\epsilon_{xx}(\mathbf{q})|^2\sin^2\delta+|\epsilon_{xy}(\mathbf{q})|^2\cos^2\delta, \qquad (21)$$

$$|g_{x,f2}(\mathbf{q})|^2 = |\epsilon_{xy}(\mathbf{q})|^2. \qquad (22)$$

Finally, from Eqs. (15) and (16) we obtain

$$I(\mathbf{q}) = I_{x,f1}(\mathbf{q})+I_{x,f2}(\mathbf{q}) = \frac{2I_0 k_0^4 \Delta m^2 V\zeta^3}{45\pi L^2\langle m\rangle^2}\frac{7-\sin^2\theta\cos^2\phi}{(1+q^2\zeta^2)^2}. \qquad (23)$$

It can be interesting to note that it is also possible to extract from Eqs. (15) and (16) the ratio between the polarized $[I_{VV}(\mathbf{q})]$ and depolarized $[I_{VH}(\mathbf{q})]$ scattering intensities when $\mathbf{k}_f$ lies in the yz plane,

$$I_{VV}(\mathbf{q})/I_{VH}(\mathbf{q})=4/3. \qquad (24)$$

From Eqs. (4) and (23), after some calculations we obtain

$$\tau=\frac{\Delta m^2}{90\langle m\rangle^2}\frac{[(1+4k_0^2\zeta^2+28k_0^4\zeta^4)4k_0^2\zeta^2-(1+6k_0^2\zeta^2+8k_0^4\zeta^4)\ln(1+4k_0^2\zeta^2)]}{k_0^2\zeta^3(1+4k_0^2\zeta^2)}. \qquad (25)$$

Equation (25) expresses the optical turbidity calculated for a FN in the BA within our model. It provides a relationship between the measured τ and the nematic correlation length ζ. In Fig. 3 we show $\tau(\zeta)$ as calculated from Eq. (25) at two different temperatures by using for k_0, Δm, and $\langle m\rangle$ the values appropriate to our experiment. Note the existence of two regimes. In the limit of large ζ, Eq. (25) transforms into

$$\tau=\frac{14k_0^2\zeta\Delta m^2}{45\langle m\rangle^2}, \quad \zeta k_0\gg 1. \qquad (26)$$

while, in the limit of short nematic correlation lengths

$$\tau=\frac{32k_0^4\zeta^3\Delta m^2}{27\langle m\rangle^2}, \quad \zeta k_0\ll 1. \qquad (27)$$

According to Eq. (26), for large ζ, τ can be arbitrarily large. This is evidently an artifact of the BA, which, for ζ larger than $\lambda/\Delta m$, is definitely inapplicable. The behavior of Eq. (26) would in fact lead to the conclusion that the bulk LC is infinitely turbid.

IV. LIGHT SCATTERING FROM A DISTORTED NEMATIC: ANOMALOUS DIFFRACTION APPROXIMATION

In this section we develop a model for the regime of large correlation lengths by using the anomalous diffraction approach. According to the ADA, the incident light travels across the sample maintaining its intensity profile, but losing its spatial coherence: the optical inhomogeneities within the system act as thin phase modulators. The phase modulation is expressed by assuming that the incident light propagates through the scattering medium as an ensemble of straight rays. Each ray then exits the sample with a phase given by the optical path experienced within the sample. In this way the scattering object does not introduce, in the near field, any variation in the intensity or in the direction of propagation. The perturbed wave front of the radiation at the exit of the sample gives rise, in the far field, to scattering (ordinary diffraction).

Our ADA model differs from the BA model of the preceding section in two respects. First, as anticipated in the preceding section, it describes the system as a collection of independent and randomly oriented uniaxial scatterers. The structure of the scatterers is chosen in such a way that the model is consistent with the statistical properties of the continuous distorted nematic texture assumed in the BA model.

Second, we calculate the total scattered intensity in our ADA model through the optical theorem [12] rather than explicitly calculating the integral in Eq. (4). This constitutes a great simplification in the calculations, which cannot be used in the BA, since in the BA the energy of the optical radiation is not conserved through the scattering process.

In order to specify the properties of the scatterers, let us take a generic point $\mathbf{r}_0$ within the sample and call $\mathbf{n}_0$ the nematic director in that point. Upon moving away from $\mathbf{r}_0$, the director increasingly loses memory of the original orientation in $\mathbf{r}_0$. Let us now consider all the locations inside the sample where the nematic director points along $\mathbf{n}_0$ and call them $\{\mathbf{r}_i\}$. Let us also consider all the orientations of the director in the positions $\{\mathbf{R}_i\}=\{\mathbf{r}_i+\mathbf{R}\}$, where $\mathbf{R}$ is an arbitrary shift. We define an average ''optical profile'' $\overline{Q_{\alpha\beta}}(\mathbf{R})$ as follows:

$$\overline{Q_{\alpha\beta}}(\mathbf{R})=\frac{1}{N}\sum_i^N Q_{\alpha\beta}(\mathbf{R}_i)$$

$$=\int Q_{\alpha\beta}(\mathbf{n}(\mathbf{R}_i))P(\mathbf{n}(\mathbf{R}_i)|\mathbf{n}(\mathbf{r}_i))d\mathbf{n}(\mathbf{R}_i)$$

$$=Q_{\alpha\beta}(\mathbf{r}_i)\exp\left(-\frac{R}{\zeta}\right), \qquad (28)$$

where N is the total number of locations $\mathbf{r}_i$ and $P(\mathbf{n}(\mathbf{r}_1)|\mathbf{n}(\mathbf{r}_2))$ is the conditional probability of a certain orientation of $\mathbf{n}$ in $\mathbf{r}_1$ given its orientation in $\mathbf{r}_2$. The integration in $d\mathbf{n}(\mathbf{R}_i)$ indicates the integration on all possible orientations of the director at the position $\mathbf{R}_i$. In Eq. (28) we have made use again of the analogy between the space dependence of the random orientation of the nematic director and time dependence of the axis of a Brownian rotator, as described in the preceding section. Since the conditional probability of the orientation of a Brownian rotator at two different times is explicitly known [14], the analogy leads to the last equality of Eq. (28).

From Eqs. (28) and (8) we obtain

$$\overline{\epsilon_{\alpha\beta}}(\mathbf{r}_i+\mathbf{R})=\langle\epsilon\rangle\delta_{\alpha\beta}+(2/3)\Delta\epsilon_s Q_{\alpha\beta}(\mathbf{r}_i)\exp\left(-\frac{R}{\zeta}\right). \qquad (29)$$

Equation (29) describes a uniaxial correlation volume, coherently aligned along $\mathbf{n}_0$. Its optical anisotropy is equal to that of bulk LC in the center, and exponentially vanishes as one moves away from its center. The surrounding medium is
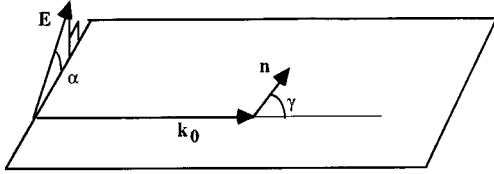
FIG. 4. Geometrical definitions of the angles α and γ, used in the ADA model. **n** lies in the plane shown in the figure. α defines the orientation of the incident polarization with respect to such a plane. γ is the angle between **n** and $\mathbf{k}_0$.

taken to be isotropic with refractive index $\langle m \rangle$. The ordinary refractive index m_o experienced by an incident ray crossing the medium, as a function of the distance R from the center of the scatterer, is

$$m_o = \langle m \rangle - \frac{1}{3} \Delta m \, \exp\left(-\frac{R}{\zeta}\right). \qquad (30)$$

Analogously, when the polarization of the incident light is parallel to $\mathbf{n}_0$, the extraordinary refractive index m_e is

$$m_e = \langle m \rangle + \frac{2}{3} \Delta m \, \exp\left(-\frac{R}{\zeta}\right), \qquad (31)$$

whereas, otherwise, for an incident ray not perpendicular to $\mathbf{n}_0$, we have

$$m_e(\gamma) = \left[\frac{\cos^2 \gamma}{m_o^2} + \frac{\sin^2 \gamma}{m_e^2}\right]^{-1/2}, \qquad (32)$$

where γ is defined in Fig. 4 as the angle between **n** and $\mathbf{k}_0$.

Since the scatterers are ''index matched,'' i.e., the refractive index away from the center of the scatterers is equal to the average refractive index in the scatterer, the amplitude of the scattered field depends only on the orientation of the optical axis. Considering that the orientation is random for distances larger than ζ, the total scattering of a system of uniaxial scatterers optically matched with the solvent is the incoherent summation of the scattering of each single scatterer [13(d)]. As a consequence, the turbidity of a FN within this approximation is simply related to the total cross section σ_0 of a single exponential scatterer, averaged over all possible orientations of its optical axis

$$\tau = C \, \frac{\langle \sigma_0 \rangle}{\zeta^3}, \qquad (33)$$

where C/ζ^3 is the number density of scatterers. At this stage C cannot be better defined. We call α the angle between the polarization of the incident light and its projection in the scattering plane (see Fig. 4). The averaged total cross section is

$$\langle \sigma_0 \rangle = \frac{1}{4\pi} \int_0^\pi \sin\gamma \, d\gamma \int_0^{2\pi} d\alpha \, \sigma_0. \qquad (34)$$

The total cross section can be calculated from the scattering amplitude in the forward direction. Because of the conservation of the total incident energy, in fact, the light scattered in the forward direction interferes with the transmitted beam so
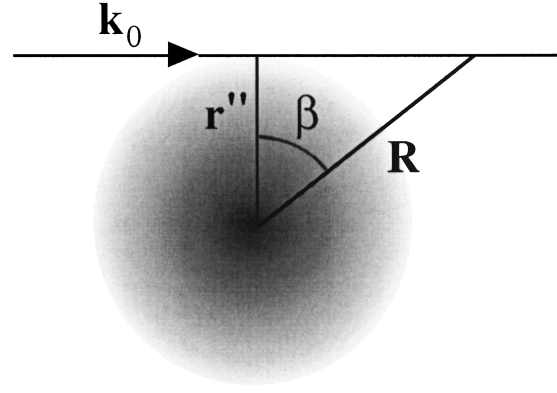
FIG. 5. Geometrical definitions of the quantities β, r'', and R, used in the ADA model. The thick line represents a light ray passing at a distance r'' from the center of the scatterer. R indicates the distance from the center of the scatterer of a generic point on the ray.

as to decrease the intensity of the transmitted beam of an amount equal to the total scattered intensity. This is the basic content of the optical theorem [12], which is expressed in the equation

$$\sigma_0 = \frac{4\pi}{k^2} \, \mathrm{Re}[\mathbf{e} \cdot \underline{S}(\underline{0}) \cdot \mathbf{e}], \qquad (35)$$

where **e** is a unit vector parallel to the polarization of the incident light,

$$\mathbf{e} = \frac{\mathbf{E}}{|\mathbf{E}|} = \begin{bmatrix} \cos \alpha \\ \sin \alpha \end{bmatrix} \qquad (36)$$

and $S(0)$ is the scattering matrix as defined by the classic treatment of van de Hulst [12].

We calculate now the scattered field by using a procedure similar to that adopted by Zumer for the case of LC droplets in a homogeneous matrix [13(b)]. We describe the incident light beam as an ensemble of parallel rays crossing the sample at a distance r'' from the center of the scattering object, as shown in Fig. 5. Defined in this way, $\mathbf{r}''$ is a vector perpendicular to $\mathbf{k}_0$. After having crossed the sample the field has a phase depending on r''. We express the diffraction contribution in the forward direction as

$$\underline{S}(\underline{0}) = k^2 \int_0^\infty [1 - \underline{P}(\underline{0})] r'' dr'', \qquad (37)$$

where the matrix $P(0)$ is given by

$$\underline{P}(\underline{0}) = \begin{bmatrix} \exp[i\Delta_e(\gamma)] & 0 \\ 0 & \exp(i\Delta_o) \end{bmatrix} \qquad (38)$$

and Δ_o and Δ_e are the phase shifts of an ordinary and an extraordinary ray with respect to a ray propagating in the absence of scatterer. Δ_o and Δ_e are given by

$$\Delta_o = \frac{k}{\langle m \rangle} \int_{-\pi/2}^{\pi/2} (m_o - \langle m \rangle) \frac{r''}{\cos^2 \beta} \, d\beta, \qquad (39)$$

$$\Delta_e(\gamma) = \frac{k}{\langle m \rangle} \int_{-\pi/2}^{\pi/2} [m_e(\gamma) - \langle m \rangle] \frac{r''}{\cos^2\beta} \, d\beta, \quad (40)$$

where β is defined in Fig. 5.

To perform the integrals in Eq. (40), we expand $m_e(\gamma)$ in powers of Δm and retain the first term only,

$$m_e(\gamma) \approx \langle m \rangle + \left(\frac{2}{3} - \cos^2\gamma\right) \exp\left(-\frac{R}{\zeta}\right) \Delta m. \quad (41)$$

We then obtain for the phase shifts

$$\Delta_o = -\frac{A}{3} \zeta b(x), \quad (42)$$

$$\Delta_e(\gamma) = \left(\tfrac{3}{2} - \cos^2\gamma\right) A \zeta b(x), \quad (43)$$

where

$$x = \frac{r''}{\zeta}, \quad (44)$$

$$A = \frac{2k}{\langle m \rangle} \Delta m, \quad (45)$$

$$b(x) = x K_{-1}(x), \quad (46)$$

where $K_1(x)$ is the modified Bessel function of the second kind. By calculating the real part of $P(0)$ and integrating with respect to x, α, and γ, we obtain

$$\tau = \frac{2\pi C}{\zeta} H(A\zeta), \quad (47)$$

where the function $H(y)$ is defined by

$$H(y) = \int_0^\infty \left[2 - \left(\frac{\pi}{2yb(x)}\right)^{1/2} G[yb(x)] - \cos\left(\frac{y}{3} b(x)\right) \right] x \, dx \quad (48)$$

and

$$G(z) = \cos\left(\frac{2z}{3}\right) C_F\left(\frac{2z}{\pi}\right)^{1/2} + \sin\left(\frac{2z}{3}\right) S_F\left(\frac{2z}{\pi}\right)^{1/2}, \quad (49)$$

where the functions $S_F(x)$ and $C_F(x)$ are the Fresnel-sine and Fresnel-cosine functions. The function $H(y)$ in Eq. (48) cannot be calculated analytically, but can be easily computed numerically. Note that all the experimental parameters are contained in the quantity A. Indeed, as shown in Eqs. (44) and (47), the quantities $\tau\zeta$ and $\tau/\Delta m$ as calculated in our ADA model are functions of the nematic correlation length and of the LC birefringence only through the product $\zeta\Delta m$. In Fig. 6 we plot $\tau\zeta$ and $\tau/\Delta m$ as functions of $\zeta\Delta m$ assuming $\lambda = 633$ nm, $\langle m \rangle = \langle m_{6CB} \rangle = 1.58$, and $C = 0.029$.

The ADA model contains the unspecified constant C. We have determined C by exploiting the fact that the ADA and BA models have an overlapping range of validity, so that we can derive C by imposing that the $\tau(\zeta)$ calculated in the ADA regime overlaps the $\tau(\zeta)$ calculated in the BA regime in an appropriate range of ζ. This is shown in Fig. 3 where we plot
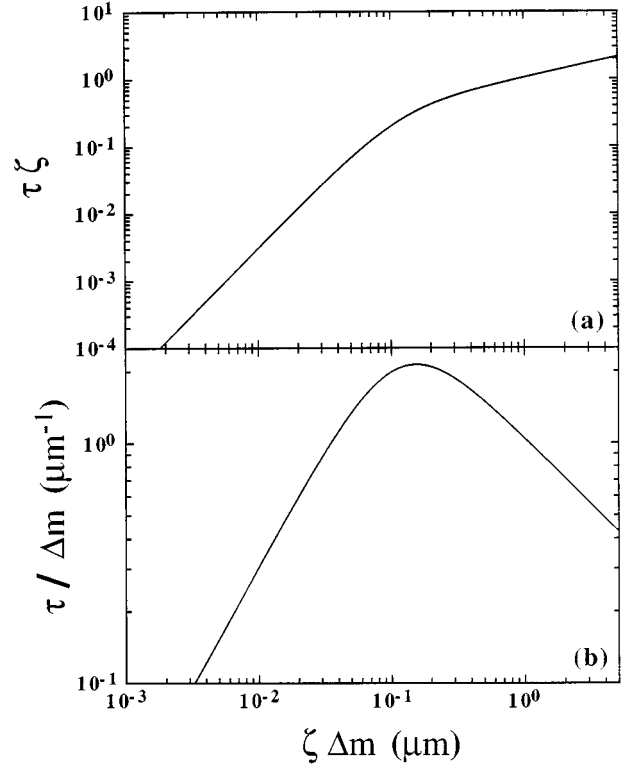
FIG. 6. Calculated values of $\tau\zeta$ (a) and $\tau/\Delta m$ (b) plotted as a function of the product $\zeta\Delta m$ according to the ADA model.

$\tau(\zeta)$ for two different temperatures, corresponding to two different local birefringences. Since the range in which the two models have overlapping $\tau(\zeta)$ is quite narrow, we have determined the scaling constant by aligning the asymptotic behavior for low ζ of the $\tau(\zeta)$ calculated in the ADA model, with the high ζ asymptotic behavior obtained in the BA. In both asymptotic limits, in fact, $\tau(\zeta) \propto \zeta$. We obtain $C \approx 0.029$. As a result, Fig. 3 defines a composite model on the whole ζ axis, which coincides with the BA model for $\zeta < 0.2$ μm, and with the ADA model for $\zeta > 0.2$ μm, $\zeta \approx 0.2$ μm being the value at which the two models coincide. Such a composite model has no free parameters. The same general features of Fig. 3, i.e., the two regimes $\tau(\zeta) \propto \zeta^3$ and the $\tau(\zeta) \propto \zeta$ obtained in the BA, and the two regimes $\tau(\zeta) \propto \zeta$ and the $\tau(\zeta) \propto \zeta^{-x}$ with $0 < x < 1$ regimes for the ADA scattering, together with the existence of an overlapping region, are also found in the much better known problem of light scattering from homogeneous particles in a homogeneous medium [12].

In Fig. 7 we show the theoretical dependence of τ on T calculated from the ADA model for different ζ. Here, again, we have used the values of $\Delta m(T)$ and $\langle m \rangle$ of bulk 6CB. Notice the striking similarity with Fig. 1. Indeed, we can distinguish a "small ζ" regime ($\zeta < 1$ μm), where τ grows with ζ and is proportional to $\Delta m^2(T)$, and a "large ζ" regime ($\zeta > 1$ μm), where the discontinuity of τ at $T = T_{NI}$ is more pronounced and the τ vs T dependence in the nematic phase is weaker.

V. THE NEMATIC CORRELATION LENGTH OF THE FILLED NEMATIC

In this section we analyze the experimental data by using the models developed in the previous two sections. Accord-
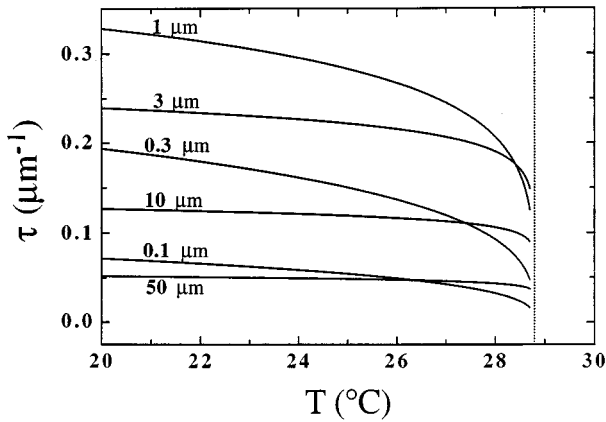
FIG. 7. Calculated values of the turbidity τ plotted as a function of the temperature T, for different values of the nematic correlation lengths ζ. The numbers labeling the curves indicate the value of ζ used to calculate $\tau(T)$.

ing to Figs. 3 and 7, the theoretical $\tau(\zeta)$ has a maximum. If we consider, for instance, $T=20$ °C, we find that the maximum value of $\tau(T=20$ °C) calculated from the model is $\tau=0.33$ μm^{-1}. It is interesting to note that the maximum turbidity which we have experimentally measured at $T=20$ °C is $\tau=0.34$ μm^{-1} (for the sample having $\phi=0.052$). The agreement between experiment and models is remarkable.

In Figs. 8(a) and 8(b), we show examples of the compari-
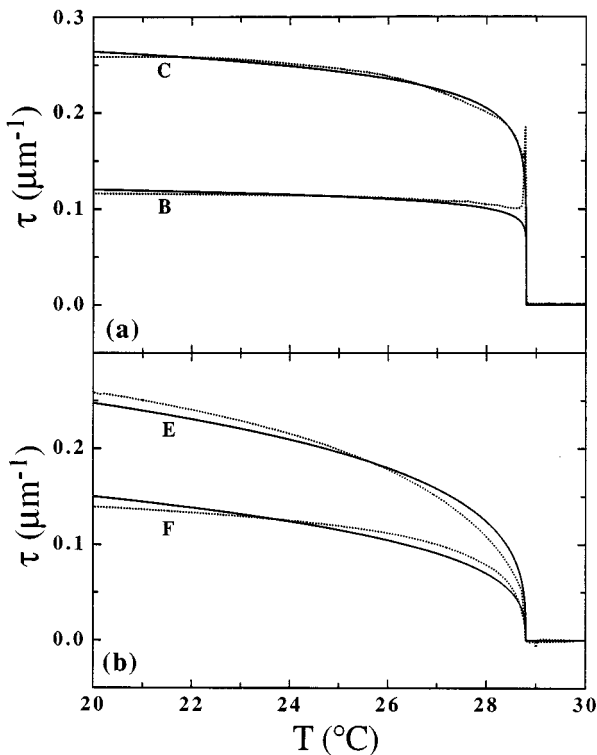
FIG. 8. Measured turbidity (dotted lines) and calculated turbidity (continuous lines) plotted as a function of the temperature T. In this figure we use the same labels as in Fig. 1. (a) Curve B: $\Phi=0.013$, $\zeta=10.4\pm0.7$ μm; curve C: $\Phi=0.026$, $\zeta=2.41\pm0.09$ μm. (b) Curve E: $\Phi=0.083$, $\zeta=0.42\pm0.02$ μm; curve F: $\Phi=0.120$, $\zeta=0.22\pm0.01$ μm.

son between the $\tau(T)$ curves shown in Fig. 1 and the theoretical $\tau(T)$ curves which fit the experimental results using ζ as the free parameter. We see that the models can reproduce reasonably well the shape of the experimental curves. It should be noted that, since $\tau(\zeta)$ has a maximum, the matching in the T dependence is necessary to uniquely extract ζ from the data. In fact, the absolute value of τ at a given T would not be sufficient to discriminate between the right and left arms of $\tau(\zeta)$ with respect to the maximum. We remark that the fitting curves in Fig. 8, which describe satisfactorily the measured $\tau(T)$ over the whole temperature range 20–28.8 °C, have been obtained by assuming one value only for the nematic correlation length ζ. Upon decreasing the temperature from the isotropic phase, there is certainly a small temperature interval where the nematic correlation length grows continuously from zero, corresponding to bulklike paranematic fluctuations. The correlation length for such fluctuations, however, does not grow to any value comparable to the value of ζ measured in the FN: in the bulk, when $T=T_{NI}$, the nematic correlation length in the isotropic phase is of the order of 100–200 Å. Quite likely, what happens in our system upon decreasing the temperature from the isotropic phase is that the nematic correlation length grows continuously as in the bulk pretransitional phenomena, then jumps to a much larger value determined by the quenched disorder. Upon further reduction of the temperature, the local orientational order and the elastic constants grow. The fact that there is no consequent growth of the nematic correlation length indicates that the coupling strength of the LC with the silica branches is strong. All these considerations cease to apply when Φ becomes so large that the discontinuity in the LC properties disappears ($\Phi\geqslant0.15$).

The discontinuous jump in the value of ζ at $T=T_{NI}$ is also at the origin of the nonequilibrium peak observed in samples having low concentration of silica. In fact, when the FN sample is cooled down through $T=T_{NI}$, the nematic order nucleates homogeneously in the sample, giving rise to a pattern of small nematic regions which then coalesce in larger domains until they reach the value of ζ imposed by the artificial disorder. Such a process is indeed the same as in bulk nematic LC, the difference being in the finite equilibrium value of ζ and also in the time scale of this dynamic evolution, much slower than the one of bulk LC. What we observe in our experiment is therefore $\tau(\zeta(t))$, $\zeta(t)$ being the time-dependent instantaneous value of the nematic correlation length. We conclude that the transient peak of the turbidity at $T=T_{NI}$ in the low Φ samples is a consequence of the existence of a maximum in $\tau(\zeta)$. This is also confirmed by the fact that samples having ζ smaller than that corresponding to the maximum τ do not show any peak at the NI transition.

The values of ζ obtained from the fit are shown in Fig. 9 as a function of Φ. We find that ζ decreases as Φ grows. By fitting that, in the experiment reported here, we have obtained a dependence of ζ on Φ which could be described by a power law $\zeta\propto\Phi^{-Y}$ with exponent $Y=1.6\pm0.2$. The spread shown in the experimental data comes probably from two facts: (i) we tested different methods to prepare the samples, (ii) we discovered that there are aging processes by which the system, over a period of some weeks, tends to phase separate in particle rich and LC rich phases.

It is interesting to compare the dependence of ζ on Φ with
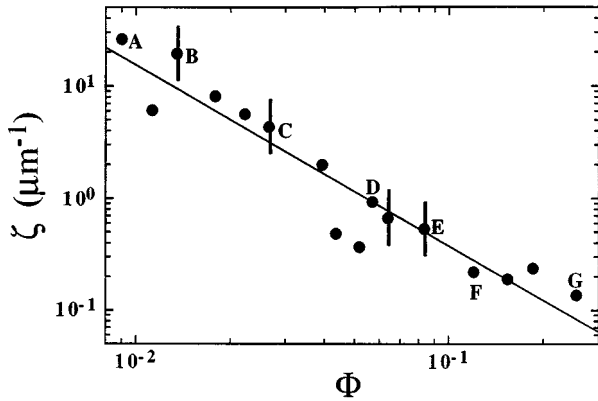
FIG. 9. Nematic correlation length ζ obtained by fitting the measured $\tau(\Phi,T)$ with the theoretical $\tau(\zeta,T)$, as a function of the volume fraction Φ of the silica particles. The labels $A-G$ refer to the curves of Fig. 1. The line indicates the power law $\zeta \propto \Phi^{-1.6}$.

the Φ dependence of the mean size of the empty cavities $\langle p \rangle$ in a colloidal gel on the concentration of the colloids. Let us assume that the colloidal aggregate has a fractal dimension d_f. We identify $\langle p \rangle$ with the fractal correlation length, i.e., with the length which is obtained from the structure factor of the aggregate as the reciprocal of the wave vector at which the q^{-d_f} behavior rolls off when q approaches zero. It is easily found that $\langle p \rangle \propto \Phi^{-1/(3-d_f)}$. We can imagine two possible scenarios. The first scenario assumes that the aggregate of silica particles in the LC resembles a colloidal aggregate in aqueous solution with $d_f \approx 2$. This would lead to $\zeta \propto \langle p \rangle^{1.6}$. This is an intriguing result, especially because it closely resembles the behavior of the smectic correlation length ξ_S obtained by studying via x-ray spectroscopy the phase behavior of a liquid crystal incorporated in silica aerogels of different densities [15]. In that context it was found that $\xi_S \propto \langle p \rangle^{1.56}$, where $\langle p \rangle$, the average pore size of the aerogel, was derived from the structure factor of the silica aerogel. This scaling behavior of the range of two different LC ordered phases as a function of the concentration of the quenched disorder does not have any explanation yet. The second scenario assumes that ζ must be proportional to the fractal correlation length: this would imply $d_f = 2.4$, indicating that the fractal structure of the aggregate is more compact than one would expect from the standard aggregation models.

In principle, Y can be theoretically obtained from the classic Imry-Ma approach [5] to the problem of the stability of the long range order to the presence of quenched disorder [16]. The Imry-Ma argument is an approximate criterion which focuses on the ordered phase of spin models and enables one to extract the size of ordered domains when an uncorrelated quenched disorder is acting on the spins. A naive and straightforward application of such a criterion would lead, however, to the result $Y = 1$. The main difference between the Imry-Ma model and our system is that the random field in the Imry-Ma model is uncorrelated, while in our experimental sample the quenched disorder is spatially correlated since it acts on the molecules in contact with the silica surface. By assuming that the random field is spatially correlated as a fractal network, the exponent Y becomes a function of the fractal dimension. Another possible difference

between the experimental situation and the Imry-Ma model is that the surface alignment of the molecules on the silica particles could be correlated to the local direction of the necklace of silica particles which form the colloidal gel. Indeed, recent works show that the interaction between particles dispersed in a liquid crystal heavily depends on the surface alignment [17]. Although the aggregation has been produced in the isotropic phase, given the fact that 6CB molecules generally prefer planar alignment when in contact with silica surfaces, one can speculate that partial reorientation of the Aerosil particles leads to a situation where the nematic director is preferentially oriented in the direction of the silica necklaces. In this case the exponent Y resulting from an Imry-Ma-like argument is further modified. All these possibilities still need to be theoretically explored.

This brief discussion shows that the measurement of $\zeta(\Phi)$ may represent an important test of the current understanding of the order-disorder phase transitions in the presence of random disorder.

Finally, it is worth noting that Eq. (47) is relevant for the technology of the FN. Equation (47), in fact, enables us to evaluate the maximum possible optical turbidity attainable in a FN. According to Eq. (47), the ratio $\tau/\Delta m$ is a function of the product $\xi\Delta m$ only. As shown in Fig. 6(b), $\tau/\Delta m$ has a maximum $(\tau/\Delta m)_{max} = 2.15$ μm^{-1}, obtained when $\xi\Delta m = 0.15$ μm. As an example, we take red light illumination and $\langle m \rangle \approx 1.5$. Therefore, by using a commercial LC optimized for nematic LC displays, having a birefringence which could be as large as 0.25, one could obtain a turbidity of $\tau_{max} = 0.54$ μm^{-1}, that is, on average, a scattering event every 2.9 wavelengths. Such a turbidity is indeed quite high, given that the shortest photon mean free path obtained in the photon localization experiments by using TiO$_2$ powders is about one wavelength [18].

VI. CONCLUSIONS

We have studied a nematic liquid crystal in which we have dispersed silica particles of nanometric size in different concentrations, ranging from 0.9% to 25% of the total volume. The result is a disordered nematic phase, where the orientation of the nematic director, and hence of the optical axis, is continuously distorted as a function of the position in the system. This composite LC-Aerosil system is highly opaque in the nematic phase, while it is almost transparent when the LC is in the isotropic phase. Since the large scattering of light in the nematic phase is due to the distortion of the optical axis of the nematic, measuring the turbidity is a way to evaluate the nematic distortions. In this paper we have shown that such an evaluation can be performed in a quantitative fashion.

We have measured the optical turbidity as a function of the temperature in samples containing different volume fractions of silica particles. We find that the temperature dependence of τ drastically changes in a nonmonotonic fashion when Φ is changed. At fixed T, $\tau(\Phi)$ has a maximum at about $\Phi = 0.055$. Moreover, when $\Phi < 0.055$, τ has a large jump at $T = T_{NI}$ and an almost constant value for lower T. On the contrary, when $\Phi > 0.055$, at $T = T_{NI}$ τ is almost continuous but it strongly depends on T. In this high Φ regime,

the τ vs T curves are all similar in shape and compare well with the T dependence of the bulk value of Δm^2.

In order to interpret these observations, we have developed a theoretical model for the scattering of light from a distorted uniaxial material. The model has been developed in two different approximations: the weak scattering approximation, valid in the regime where $\Delta m \ll 1$ and $\zeta \Delta m \ll \lambda$, and the anomalous diffraction approximation, valid instead when $\Delta m \ll 1$ and $\zeta \gg \lambda$. The two regimes together cover the whole ζ axis. The common ground for the development of the two models is represented by two main assumptions: (i) the local birefringence of the LC is equal to the bulk Δm, (ii) the fourth-order correlation functions for the orientation of the nematic director can be expressed in terms of second-order correlations. While these assumptions are sufficient to develop the BA model, in the ADA calculation we had to make a more drastic simplification: we have assumed that our system is a collection of independent anisotropic scatterers with continuous optical profile. By matching the two models in the common range of validity, we have obtained a composite model which permits us to calculate $\tau(\zeta, T)$ over the whole ζ axis, with no free parameters. By fitting the experimental $\tau(\Phi, T)$ with the theoretical $\tau(\zeta, T)$, we could extract ζ as a function of Φ. The quality of the fit is quantitatively very good, indicating that our model successfully captures the physics beyond the observed optical properties of our composite system.

The obtained dependence of ζ on Φ can be described by a power law $\zeta \propto \Phi^{-Y}$ with exponent $Y \approx 1.60$. By assuming that the aggregates of silica particles in the LC are fractals with dimension 2, our experimental results imply $\zeta \propto \langle p \rangle^{1.6}$, where $\langle p \rangle$ is the mean size of the pores within the aggregate. This result is analogous to the one obtained by studying disordered smectics. By following a different path, Y could be theoretically obtained from the classic Imry-Ma approach to the problem of the stability of the long range order in the presence of quenched disorder. A naive and straightforward application of such a criterion would lead to $Y = 1$. This fact indicates that either the quenched disorder present in our system cannot be modeled as uncorrelated, or that the approximations beyond the Imry-Ma approach are too strong. We conclude that the measure of $\zeta(\Phi)$ is an important experimental test of the current understanding of the order-disorder phase transitions in the presence of random disorder.

[1] M. Kreuzer and R. Eidenschink, in *Liquid Crystals in Complex Geometries*, edited by G. P. Crawford and S. Zumer (Taylor & Francis, London, 1996), Chap 15.

[2] B. Zhou, G. S. Iannacchione, C. W. Garland, and T. Bellini, Phys. Rev. E **55**, 2962 (1997).

[3] A. Maritan, M. Cieplak, T. Bellini, and J. R. Banavar, Phys. Rev. Lett. **72**, 4113 (1994).

[4] T. Ushida and H. Seki, in *Liquid Crystals. Applications and Uses*, edited by B. Bahadur (World Scientific, Singapore, 1990), Vol. 3, Chap. 5; X. Zhuang, D. Wilk, L. Marrucci, and Y. R. Shen, Phys. Rev. Lett. **75**, 2144 (1995).

[5] Y. Imry and S.-K. Ma, Phys. Rev. Lett. **35**, 1399 (1975).

[6] (a) P. P. Karat and N. V. Madhusudana, Mol. Cryst. Liq. Cryst. **36**, 51 (1976); (b) H. J. Coles and C. Strazielle, *ibid.* **55**, 237 (1979); (c) N. V. Madhusudana and R. Pratibha, *ibid.* **89**, 249 (1982).

[7] P. G. de Gennes and J. Prost, *The Physics of Liquid Crystals* (Oxford, Oxford, 1993).

[8] E. M. Averyanov, V. A. Zhuikov, V. Ya. Zyryanov, and V. F. Shabanov, Zh. Eksp. Teor. Fiz. **86**, 2111 (1984) [Sov. Phys. JETP **59**, 1227 (1985)].

[9] Degussa AG, Frankfurt/M., Technical Bulletin Pigments, Institution Report No. 11, 1984.

[10] *Liquid Crystals in Complex Geometries*, edited by G. P. Crawford and S. Zumer (Taylor & Francis, London, 1996).

[11] T. W. Stinson and J. D. Litster, Phys. Rev. Lett. **25**, 503 (1970); T. W. Stinson, J. D. Litster, and N. A. Clark, J. Phys. (Paris), Colloq. **33**, C1-69 (1972).

[12] H. C. van de Hulst, *Light Scattering by Small Particles* (Dover, New York, 1981).

[13] (a) S. Zumer and J. W. Doane, Phys. Rev. A **34**, 3373 (1986); (b) S. Zumer, *ibid.* **37**, 4006 (1988); (c) T. Bellini, N. A. Clark, C. D. Muzny, C. W. Garland, D. W. Schaefer, and B. J. Oliver, Phys. Rev. Lett. **69**, 788 (1992); (d) V. Degiorgio, R. Piazza, T. Bellini, and M. Visca, Adv. Colloid Interface Sci. **48**, 61 (1994); (e) T. Bellini and N. A. Clark, in *Liquid Crystals in Complex Geometries*, edited by G. P. Crawford and S. Zumer (Taylor & Francis, London, 1996), Chap. 19.

[14] B. J. Berne and R. Pecora, *Dynamic Light Scattering* (Krieger, Malabar, 1990), Chaps. 3 and 7.

[15] A. G. Rappaport, B. N. Thomas, N. A. Clark, and T. Bellini, in *Liquid Crystals in Complex Geometries*, edited by G. P. Crawford and S. Zumer (Taylor & Francis, London, 1996), Chap. 20.

[16] A. Maritan (private communication).

[17] P. Poulin, H. Stark, T. C. Lubensky, and D. A. Weitz, Science **275**, 1770 (1997); R. W. Ruhwandl and E. M. Terentjev, Phys. Rev. E **55**, 2958 (1997).

[18] D. S. Wiersma, M. P. van Albada, B. A. van Tiggelen, and A. Lagendijk, Phys. Rev. Lett. **74**, 4193 (1995).